# STRESS-STRAIN RELATIONS FOR DRY AND SATURATED SANDS
# PART I: INCREMENTAL MODEL

ANDRZEJ SAWICKI
WALDEMAR ŚWIDZIŃSKI

*Institute of Hydro-Engineering, IBW PAN, Gdańsk-Oliwa, Poland*
*e-mail: as@ibwpan.gda.pl; waldek@ibwpan.gda.pl*

The incremental model describing the pre-failure behaviour of granular soils is proposed. Firstly, the constitutive equations are derived from the extensive set of experimental data, for the triaxial configuration. The following features are included into the model: initial anisotropy, initial state of sand (i.e. either dilative or contractive), instability line. Then, the incremental constitutive equations are generalized to the 3D case, using techniques of tensor algebra. Finally, the model is re-derived for the undrained conditions in order to predict such phenomena as, for example, static liquefaction. The approach presented is an alternative to already classical approaches as the elasto-plasticity or hypoplasticity. The paper consists of two parts. Part I deals with the formulation of the model and its calibration, whereas Part II is devoted to verification of the model against experimental results.

*Key words:* granular soils, stress-strain characteristics, pre-failure behaviour, instability, liquefaction, anisotropy

## 1. Introduction

This paper consists of two parts. The first one deals with the incremental model describing the pre-failure behaviour of sand both dry (or saturated and fully drained) and water saturated in undrained conditions. In the second part, various predictions of the model proposed are computed and then compared with experimental results.

The basic idea of this paper is to propose a model that has a possibly simple mathematical structure, and that is firmly based on a solid empirical background. The model is presented in the form of incremental equations,

describing the volumetric and deviatoric deformations of the soil as functions of the mean stress and the stress deviator. These equations are formulated explicitly for the conditions corresponding to triaxial tests, in the invariant form. Then, a 3D generalization of these incremental equations is presented, that takes into account the initial anisotropy of sand.

The model proposed is an alternative to already accepted approaches as, for example, the elasto-plasticity or hypoplasticity, see Kolymbas (2000a), Zienkiewicz *et al.* (1999). A natural question seems to be: why to develop alternatives to already existing tens, or perhaps hundreds, of various models of soils? Geotechnical engineers expect that theoretical models of soils would enable various analyses of practical importance, but in practice these models often fail. They even lead to wrong predictions at the elementary levels as, for example, triaxial tests, see Saada and Bianchini (1989). For these reasons, even some extreme opinions have been published. For example: "Constitutive relations is a phrase which commands respect in the Universities and revulsion in practice, and which damages both", Bolton (2001). Or: "The main shortcoming in the field of constitutive modelling is that each researcher (or group of researchers) is developing his own constitutive model. This model is in most cases very intricate and, thus, non-relocative, i.e. no other researcher is able to work with it. I can report from my own experience that it took me several months and hard work until I realized that I was unable to obtain anything with a constitutive model proposed by a colleague", Kolymbas (2000b).

The research presented in this paper is based on an extensive set of experimental data obtained and collected for many years at the Institute of Hydro-Engineering in Gdańsk. A few of the already existing approaches have been applied to describe that empirical material, but with rather limited success, see Sawicki (2003), Głębowicz (2006). Therefore, it was decided to apply a rather straightforward approach that is based on the analysis of various stress-strain curves obtained from the triaxial compression tests for different initial states of soil samples and different stress paths.

The following methodology has been applied:

a) The basis for modelling is the extensive set of experimental data obtained at the Institute of Hydro-Engineering in Gdańsk, using advanced laboratory equipment and technology. The details are described in Section 3 of the present paper.

b) The stress-strain curves corresponding to some simple loading/unloading paths, as isotropic compression and deviatoric loading at constant mean stress, were then analysed in detail. It was found that some of the experimental results can be represented as common plots, when new variables

are introduced. Then, analytical approximations of these curves were found in the form of possibly simplest functions. These approximations are different for initially contractive and dilative states of soil, and different for loading and unloading. A specific definition of the loading and unloading was proposed. It was also found that the sand investigated displays anisotropic behaviour and this feature was taken into account in the theoretical description of experimental results.

c) Incremental constitutive equations, for the triaxial configuration, were then formulated on the basis of analytical approximations of basic empirical results. The calibration of these equations has already been done in the form of analytical approximations of experimental results, as described previously. Then, the incremental equations formulated for the triaxial tests configuration, were generalized to the 3D form, using the formalism of tensor functions.

d) The incremental constitutive equations, derived for fully drained conditions, are then applied to describe the stress paths for the case of undrained conditions.

e) In Part II of this paper, various predictions of the model are examined in order to verify the incremental constitutive equations proposed. These predictions are obtained by integration of the incremental equations along the stress paths that are different from those applied for calibration. The predictions deal with the pre-failure behaviour of sand for both fully drained and undrained conditions. The results of computations are compared with respective experimental results. It is shown that the model gives quite good predictions of the pre-failure behaviour of sand.

The advantages of the methodology applied in this paper can be summarized as follows:

- Theoretical description of the pre-failure behaviour of sand is based on the extensive set of experimental data obtained at the same laboratory in similar conditions and on the same sand. For the above reason, the data presented can also be used by other researchers, in order to validate their models. Note that quite often the modelers use various empirical data, dispersed in the literature, and obtained in various laboratories at different conditions and materials, for validation of their models.

- The model is defined in possibly the simplest form that enables its application to various loading paths. The functions appearing in the incremental equations are determined directly from experimental data. The

shape of these functions can be modified, if necessary, in order to obtain better predictions.

- Some important effects are incorporated into the model proposed as, for example, the initial state of the soil (either compressive or dilative), initial anisotropy and the instability line. These effects are often ignored in the existing models. The important feature of the model is that it predicts the undrained behaviour of soil as, for example, static liquefaction, on the basis of the behaviour of fully drained soil.

## 2. Definitions

### 2.1. Stresses and strains in triaxial compression

The experimental results presented in this paper were obtained from tests performed in the triaxial apparatus enabling measurement of local strains, both the vertical and horizontal ones. During such tests, the cylindrical soil sample is subjected to the vertical and horizontal stresses, designated as $\sigma_1$ and $\sigma_3$, respectively, see Fig. 1. The corresponding strains are denoted as $\varepsilon_1$ and $\varepsilon_3$. In the case of water saturated soil, the effective stresses are defined as $\sigma' = \sigma_1 - u$, and $\sigma'_3 = \sigma_3 - u$, where $u$ denotes the pore pressure. The soil mechanics sign convention is used, where the plus sign denotes compression. Experimental results will be interpreted in terms of the following stress and strain variables

$$p' = \frac{1}{3}(\sigma'_1 + 2\sigma'_3) \qquad q = \sigma'_1 - \sigma'_3 = \sigma_1 - \sigma_3$$
$$\varepsilon_v = \varepsilon_1 + 2\varepsilon_3 \qquad \varepsilon_q = \frac{2}{3}(\varepsilon_1 - \varepsilon_3) \tag{2.1}$$

where: $p'$ is the mean effective stress; $q$ – stress deviator; $\varepsilon_v$ – volumetric strain; $\varepsilon_q$ – deviatoric strain. These variables are related directly to the stress and strain invariants

$$p' = \frac{1}{3}\operatorname{tr}\boldsymbol{\sigma}' \qquad q = \sqrt{3J_2} \qquad J_2 = \frac{1}{2}\operatorname{tr}(\boldsymbol{\sigma}'^{dev})^2$$
$$\varepsilon_v = \operatorname{tr}\boldsymbol{\varepsilon} \qquad \varepsilon_q = \sqrt{\frac{4}{3}K_2} \qquad K_2 = \frac{1}{3}\operatorname{tr}(\boldsymbol{\varepsilon}^{dev})^2 \tag{2.2}$$

where $p'$ is the first invariant of the effective stress tensor; $J_2$ – second invariant of the stress deviator; $\varepsilon_v$ – first invariant of the Cauchy strain tensor; $K_2$ – second invariant of the strain deviator.

Deviators of the tensors appearing in Eqs. $(2.2)_{3,6}$ are defined as follows

$$\boldsymbol{\sigma}'^{dev} = \boldsymbol{\sigma}' - \left(\frac{1}{3}\operatorname{tr}\boldsymbol{\sigma}'\right)\mathbf{1} \qquad \boldsymbol{\varepsilon}^{dev} = \boldsymbol{\varepsilon} - \left(\frac{1}{3}\operatorname{tr}\boldsymbol{\varepsilon}\right)\mathbf{1} \qquad (2.3)$$

The non-dimensional stress variable $\eta$ is defined as

$$\eta = \frac{q}{p'} \qquad (2.4)$$

## 2.2. Characteristic objects

Figure 1 shows two important objects represented by straight lines in the stress space $p'$, $q$, namely the Coulomb-Mohr failure condition (CM) and the instability line (IL). The failure condition is defined as follows

$$q = \frac{6\sin\phi}{3 - \sin\phi}p' = \Phi p' \qquad (2.5)$$

where $\phi$ is the angle of internal friction.

The instability line is given by the relation

$$q = \Psi p' \qquad (2.6)$$

where $\Psi < \Phi$ is a parameter which should be determined experimentally.
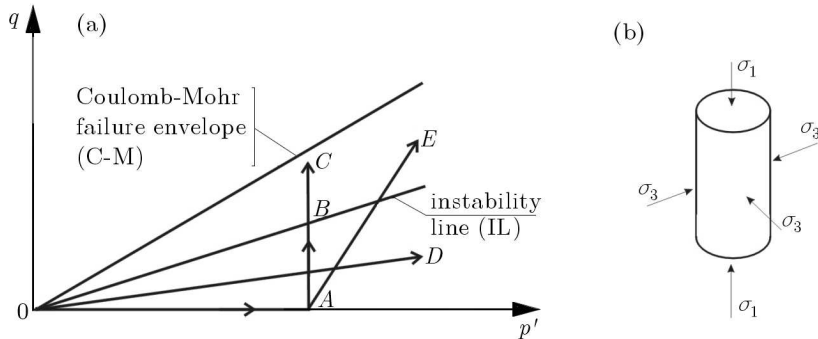


Fig. 1. Coulomb-Mohr failure condition and the instability line in the effective stress space; simple stress paths (a); stresses acting on cylindrical soil sample (b)

The instability line divides the regions of contraction and dilation of initially dilative sand subjected to pure shearing. Stress path AB corresponds to compaction, BC to dilation. These phenomena, characteristic for granular materials, take place in dry or saturated, but in free draining conditions, sands. In the case of initially contractive soil, there is no dilation along the

path ABC, just only compaction. But in undrained shearing of contractive sand, the instability line corresponds to the maximum shear stress that can be supported by the material.

The initial state of the soil is defined by a pair of numbers $e$ and $p'$, where $e$ is the initial void ratio which represents a point in the $e$, $p'$ space (in semi-logarithmic scale). This space is divided into two parts by the steady state line (SSL), see Fig. 2. The region above this line represents the states corresponding to the conctrative behaviour during shearing, whilst the states below this line correspond to the dilative behaviour. The steady state of deformation is defined as continuous flow of a granular medium at constant volume and constant stress, see Poulos (1981). We shall identify the steady state with the CM line in the effective stress space. The stress-strain characteristics of initially dilative and contractive soils differ essentially, as will be shown in subsequent sections.
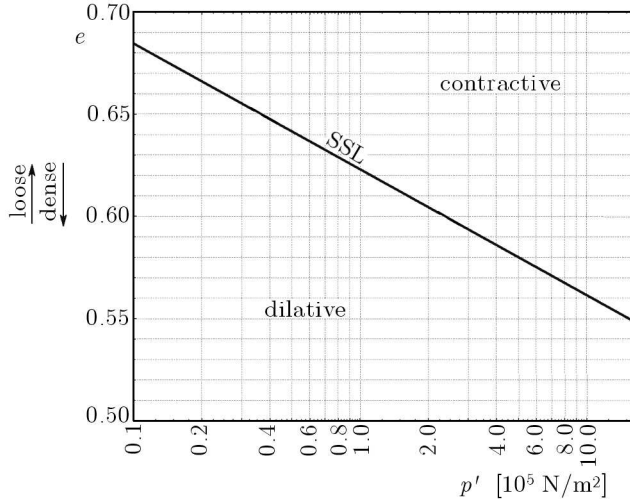


Fig. 2. Steady state line for "Skarpa" sand

### 2.3. Loading and unloading

The problem of loading and unloading has the fundamental meaning in the theory of plasticity, also with applications to soil mechanics. According to common understanding, during loading the irreversible (plastic) strains develop, whilst during unloading the reversible (elastic) strains are recovered. The problem of loading and unloading is obvious in the uni-axial case, but in a general 3D case is controversial, see Życzkowski (1973).

In classical elasto-plasticity, the definition of loading and unloading is clear. The loading takes place when the stress increment is directed outwards of the current yield surface. When it is directed inwards this surface, the process of unloading occurs. This means that the same stress increment may be associated with the loading in one theory, and in the other with unloading, see Sawicki (2003). In order to avoid such an ambiguity, we have introduced the following definitions of loading and unloading:

$dp' > 0$ – spherical loading; $\quad dp' < 0$ – spherical unloading;

$dq > 0$ – deviatoric loading; $\quad dq < 0$ – deviatoric unloading,

where $d(\cdot)$ denotes the increment of respective quantity.

It will be shown later that it is convenient to present some of the experimental data in terms of the variable $\eta$, defined in Eq. (2.4). The differential of this variable is the following

$$d\eta = \frac{\partial \eta}{\partial p'}dp' + \frac{\partial \eta}{\partial q}dq = \frac{1}{p'}(dq - \eta dp') \qquad (2.7)$$

The deviatoric loading takes place when $d\eta > 0$, and unloading is associated with the condition $d\eta < 0$, which is an alternative formulation. Figure 3 shows graphical interpretation of these conditions.
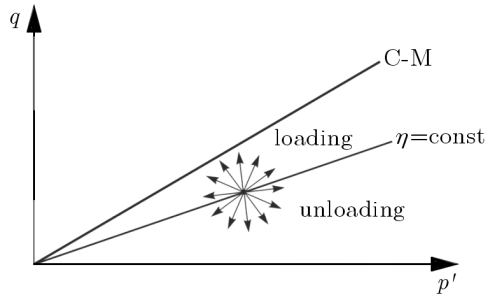


Fig. 3. Stress increments above the line $\eta = \text{const}$ define the deviatoric loading. Unloading corresponds to the stress increments directed below this line

In the special case of $\eta = \text{const}$, there is $d\eta = 0$, and the loading takes place when $dp' > 0$ and $dq > 0$, and the unloading occurs when $dp' < 0$ and $dq < 0$.

## 2.4. Useful units

For practical purposes it is convenient to introduce the following stress and strain units: stress unit $= 10^5 \, \text{N/m}^2 = 0.1 \, \text{MPa}$; strain unit $10^{-3}$ (non-dimensional).

This means that the stresses will be presented as non-dimensional quantities as, for example, $p'$ – real mean effective stress/stress unit, etc. Similarly, $\varepsilon_v$ – real volumetric strain/strain unit. The reason for introducing such units is that these quantities, i.e. stresses and strains, will be of similar order of magnitude, which is important in numerical calculations.

## 3.    Experimental investigations

### 3.1.    Methodology and experimental background

All the experiments discussed in the present paper were performed in the computer-controlled triaxial apparatus, manufactured by GDS Instruments, see Menzies (1988), Świdziński and Mierczyński (2002). The measuring system was equipped with special gauges enabling the local measurement of both the vertical and lateral strains. In the case of saturated and fully drained samples, the change of volume of pore water was also measured, which enables independent control of strains.

The experiments were performed on the quartz sand "Skarpa", characterised by the following parameters: median size of grains $D_{50} = 420\,\mu$m; uniformity coefficient $C_U = 2.5$, specific gravity $G = 2.65$; maximum and minimum void ratios $e_{max} = 0.677$ and $e_{min} = 0.432$, respectively; angles of internal friction of loose and dense sand $\phi = 34°$ and $41°$, respectively (determined from triaxial compression tests). The soil samples were prepared in a membrane-lined split moulder, ether by moist tamping or by water pluviation methods. The first method assured an achievement of very loose samples displaying the contractive behaviour at a relatively low mean effective stress level, whereas the second, uniformity of dense samples, exhibiting a dilative character during shearing.

The basic set of experiments included the isotropic loading and unloading of soil samples (paths $OA$ and $AO$, respectively, see Fig. 1), and the shearing at a constant mean stress (paths $ABC$ and $CBA$ in Fig. 1, for loading and unloading, respectively). The experiments were performed for initially loose and dense samples (isotropic compression), and for initially contractive and dilative samples (shearing at constant mean stress). The deviatoric loading/unloading experiments were performed for various values of the constant mean stress.

The experiments described above have served for calibration of the incremental constitutive equations. The stress paths $OA$ and $ABC$ for loading, and $CBA$ and $AO$ for unloading, were chosen for traditional reasons, as the sphe-

rical and deviatoric parts of respective tensors play the basic role in mechanics of materials. The experimental programme has also included the investigations of the soil samples subjected to other loading histories as, for example, paths $OAE$ or $OD$ in Fig. 1, but these results will be presented in the second part of this paper, in connection with validation of the incremental constitutive equations proposed.

### 3.2. Stress-strain curves for isotropic compression

Figure 4 shows the character of stress-strain curves during the isotropic loading and unloading (path $OAO$ in Fig. 1). The shape of these curves is similar for initially loose and dense samples. Note that during the isotropic compression, we do not consider whether the sample is either dilative or contractive, as all the samples densify in this case.
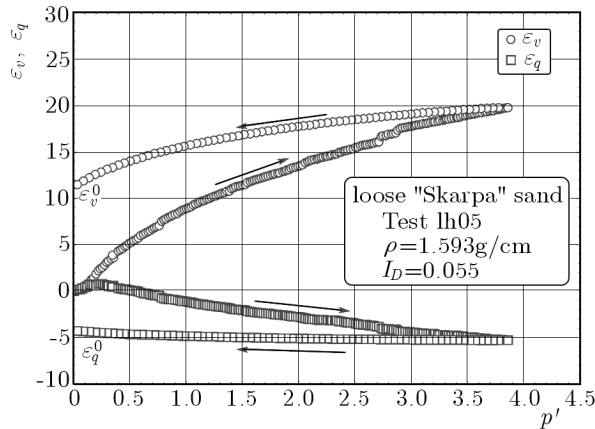


Fig. 4. Strains developed during the isotropic loading and unloading (path $OAO$ in Fig. 1). Recall respective stress and strain units, Section 2.4

It should be noted that during the isotropic compression, both the volumetric and deviatoric strains develop. In the case of initially isotropic soil, there should be $\varepsilon_q = 0$, so the samples investigated display an anisotropic character. The degree of initial anisotropy, i.e. the ratio $|\varepsilon_q/\varepsilon_v|$, is about 0.15. It was almost impossible to obtain initially isotropic samples, even using a very careful method of sample preparation in laboratory conditions. Note that most of the existing models of soils assume the initial isotropy. In this paper, the effect of initial anisotropy will be taken into account. The volumetric and deviatoric strains that develop during loading can be approximated by the following formulae

$$\varepsilon_v = A_v \sqrt{p'} \qquad\qquad \varepsilon_q = A_q \sqrt{p'} \qquad\qquad (3.1)$$

where $A_v$ and $A_q$ are coefficients the values of which depend on the initial state of sand, i.e. loose or dense. Table 1 shows the values of these coefficients, determined for two groups of samples, designated as initially loose and dense.

**Table 1.** Coefficients $A_v$ and $A_q$

| Initial state | Number of exper. | Range of density index $I_D$ | Range of $A_v$ | Average $A_v$ | Range of $A_q$ | Average $A_q$ |
|---|---|---|---|---|---|---|
| Loose | 23 | 0.016-0.445 | 3.73-7.32 | 6.01 | $-1.67$--$0.29$ | $-0.95$ |
| Dense | 26 | 0.707-0.859 | 2.23-4.54 | 3.47 | $-1.02$--$0.12$ | $-0.53$ |

Recall that the values of coefficients, presented in Table 1, correspond to the stress and strain units introduced in Section 2.4. For example, calculate the volumetric strain corresponding to $A_v = 4$ and $p' = 200\,\text{kPa} = 2 \cdot 10^5\,\text{N/m}^2$. Eq. $(3.1)_1$ gives: $\varepsilon_v = 4\sqrt{2} = 5.66$ in unit $10^{-3}$. That means that the volumetric strain is $5.66 \cdot 10^{-3} = 0.00566$.

The functions approximating experimental results may be chosen in other form than that in Eqs. (3.1). For example, instead of the square root approximation, on can apply alternatively the logarithmic or polynomial functions. It is a matter of convenience as all of those functions approximate sufficiently well the experimental results. The square root approximation was chosen for two reasons. Firstly, there appears only a single coefficient. Secondly, in geotechnical engineering, the square root approximation is applied quite often. For example, Eq. $(3.1)_1$ can be re-written as $p' = (\sqrt{p'}/A_v)\varepsilon_v$, where $\sqrt{p'}/A_v$ plays the role of the bulk modulus.

Similar approximations can be applied for the unloading curves

$$\varepsilon_v = \varepsilon_v^0 + A_v^u \sqrt{p'} \qquad\qquad \varepsilon_q = \varepsilon_q^0 + A_q^u \sqrt{p'} \qquad\qquad (3.2)$$

where $A_v^u$ and $A_q^u$ are respective coefficients, and $\varepsilon_v^0$ and $\varepsilon_q^0$ denote residual (plastic) strains that remain in the soil sample after unloading, see Fig. 4. Their values depend on the maximum value of $p'$ applied to the sample. For initially loose samples $(0.02 \leqslant I_D \leqslant 0.44)$, the average values of these coefficients are $A_v^u = 4.41$ and $A_q^u = -0.447$. For initially dense samples $(0.71 \leqslant I_D \leqslant 0.86)$, there is: $A_v^u = 2.91$ and $A_q^u = -0.205$.

### 3.3. Shearing at constant mean stress – dilative soil

Shearing at a constant mean stress is realised on the stress paths $ABC$ (loading) and $CBA$ (unloading), see Fig. 1. In this case, the response of sand

(stress-strain curves) depends strongly on its initial state, i.e. dilative or contractive, and therefore should be considered separately. Figure 5 shows the shear stress – volumetric strain curves of initially dilative samples, for various values of the mean effective stress that was kept constant during each of experiment.
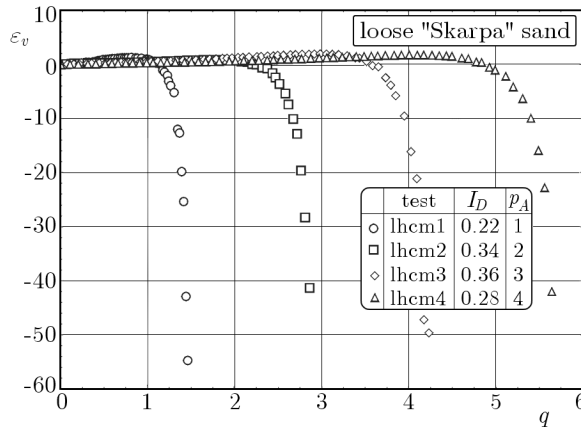


Fig. 5. Volumetric strains that develop during shearing along path $ABC$, cf. Fig. 1, for initially dilative sand and different values of $p' = const$ ($p_A$ [$10^5 \, \text{N/m}^2$])

The stress-strain curves from Fig. 5 have been re-normalised in order to present these experimental results in the form of a single common curve. The method of trial and error was applied to find such a single curve. Figure 6 shows that a useful interpretation of the experimental results can be presented using new variables, namely: $\eta$ and $\varepsilon_v/\sqrt{p'}$. Figure 6 shows the results from Fig. 5 in the form of a common curve.

The curve presented in Fig. 6 displays some interesting features of the sand behaviour. In the first stage of shearing, the sand densifies ($0 \leqslant \eta \leqslant \eta'$). The non-dimensional stress $\eta = \eta'$ corresponds to the instability line, see Eq. (2.6). Then, the process of dilation takes place. The value of $\eta = \eta''$ corresponds to the Coulomb-Mohr yield criterion, see Eq. (2.5). The curve shown in Fig. 6 can be approximated by the following formulae

$$\frac{\varepsilon_v}{\sqrt{p'}} = \begin{cases} a_1\eta^2 + a_2\eta & \text{for} \quad 0 \leqslant \eta \leqslant \eta' \\ (a_3\eta^2 + a_4\eta + a_5)[\exp(a_6\eta) - 1] & \text{for} \quad \eta' \leqslant \eta \leqslant \eta'' \end{cases} \qquad (3.3)$$

where $a_i$, $i = 1, ..., 6$, are some coefficients, which should assure the continuity of functions (3.3) at $\eta = \eta'$ as well as continuity of the first derivative which equals zero at $\eta = \eta'$. The following values of these coefficients have been
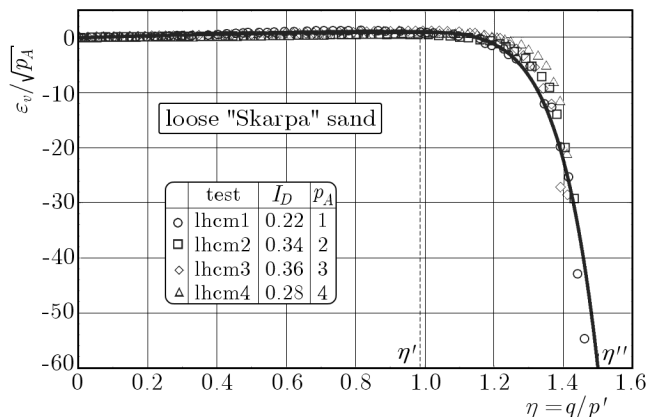
Fig. 6. Experimental results from Fig. 5 presented in the form of a single common curve ($p_A$ [$10^5$ N/m$^2$])

obtained for the experimental data: $a_1 = -1$; $a_2 = 2$; $a_3 = 4.07 \cdot 10^{-6}$; $a_4 = -9.44 \cdot 10^{-3}$; $a_5 = -1.09 \cdot 10^{-2}$, $a_6 = 6.54$.

The deviatoric strains that develop during pure shearing of dilative sand can also be represented in the form of a common curve as shown in Fig. 7. The analytical approximation of this curve is the following

$$\frac{\varepsilon_q}{\sqrt{p'}} = b_1[\exp(b_2\eta) - 1] \tag{3.4}$$

where $b_1 = 3.35 \cdot 10^{-4}$ and $b_2 = 8.32$ for the experimental data analysed (recall respective units!). For very dense sand, the respective coefficients obtained are $b_1 = 3.5 \cdot 10^{-4}$ and $b_2 = 6.648$.

### 3.4. Shearing at constant mean stress – contractive soil

The qualitative character of deviatoric strains is similar to that presented in Fig. 7. For the experimental data analysed the respective coefficients are following: $b_1 = 0.023$ and $b_2 = 6.245$. In the case of volumetric deformations, the experimental results can also be presented in the form of a single curve, as shown in Fig. 8. The respective analytical approximation of this curve is the following

$$\frac{\varepsilon_v}{\sqrt{p'}} = c_1\eta^4 \tag{3.5}$$
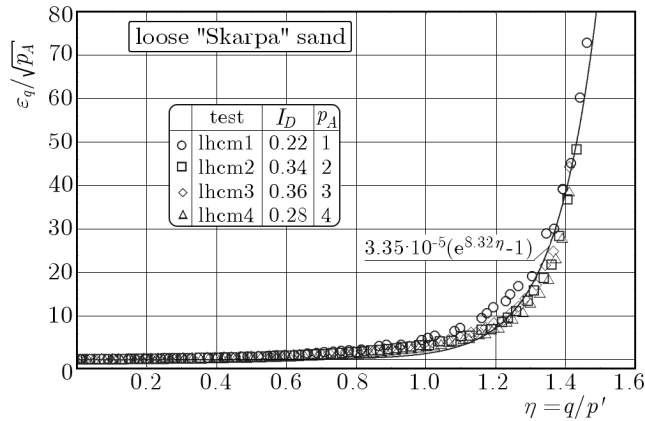
where $c_1 = 2.97$ for the data analysed.

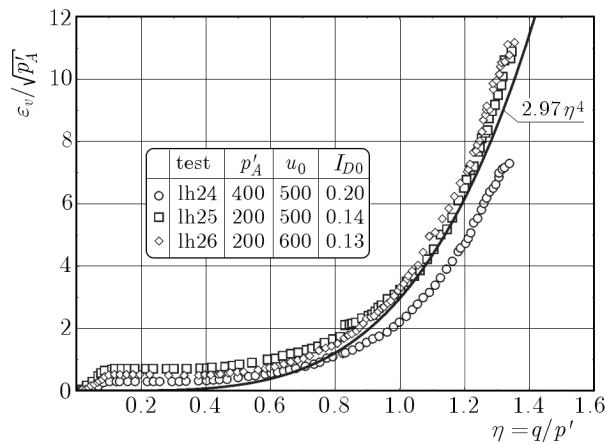Fig. 7. Common curve for deviatoric strains of initially dilative sand ($p_A$ $[10^5\,\mathrm{N/m^2}]$)



Fig. 8. Common curve for volumetric strains that develop during pure shearing of initially contractive sand

## 4.    Incremental equations for triaxial configuration

The experimental results presented in Section 3 will be generalized in the form of incremental constitutive equations. Their general form is the following

$$d\varepsilon_v = Mdp' + Ndq \qquad\qquad d\varepsilon_q = Pdp' + Qdq \qquad\qquad (4.1)$$

where $M$, $N$, $P$, $Q$ are certain functions, which will be determined from analytical approximations of the experimental results presented in Section 3. Note that the structure of Eqs. (4.1) displays some features characteristic for granular soils. Firstly, the function $N$ describes the phenomenon of dilation, i.e.

the change of volume due to shearing. For most of engineering materials as, for example, metals, concrete or plastics, there should be $N = 0$. Secondly, the function $P$ shows that the soil is initially anisotropic, as in the case of isotropy there should be $P = 0$.

The functions $M$, $N$, $P$ and $Q$ will be determined by differentiation of respective analytical approximations, as is described below. Consider the loading along the path $OA$, where the strains are approximated by Eqs. (3.1). Also note that along this paths there is $dq = 0$. Differentiation of these equations leads to the following formulae

$$d\varepsilon_v = \frac{A_v}{2\sqrt{p'}}dp' = Mdp' \qquad\qquad d\varepsilon_q = \frac{A_q}{2\sqrt{p'}}dp' = Pdp' \qquad (4.2)$$

A similar technique is applied in order to derive respective functions from the data corresponding to the path $ABC$, where $dp' = 0$. For example, consider function $(3.3)_1$. Respective differentiation leads to

$$d\varepsilon_v = \frac{\partial \varepsilon_v}{\partial \eta}\frac{\partial \eta}{\partial q}dq = \frac{1}{\sqrt{p'}}(2a_1\eta + a_2)dq = Ndq \qquad (4.3)$$

for $0 \leqslant \eta \leqslant \eta'$, etc.

Table 2 summarises all the functions for the case of loading, separately for the initially contractive and dilative sand. The values of respective coefficients, for "Skarpa" sand, are presented in Section 3.

**Table 2.** Functions appearing in Eqs. (4.2) for the case of loading

| Function | Contractive | Dilative |
|:---:|:---:|:---:|
| $M$ | | $\dfrac{A_v}{2\sqrt{p'}}$ |
| $N$ | $\dfrac{4c_1\eta^3}{\sqrt{p'}}$ | $\dfrac{1}{\sqrt{p'}}(2a_1\eta + a_2) \quad \text{for} \quad 0 \leqslant \eta \leqslant \eta',$ $\dfrac{1}{\sqrt{p'}}\{\exp(a_6\eta)[a_3a_6\eta^2 + (2a_3 + a_4a_6)\eta + a_4+$ $+a_5a_6] - 2a_3\eta - a_4\} \quad \text{for} \quad \eta' \leqslant \eta \leqslant \eta''$ |
| $P$ | | $\dfrac{A_q}{2\sqrt{p'}}$ |
| $Q$ | | $\dfrac{b_1b_2}{\sqrt{p'}}\exp(b_2\eta)$ |

Note that there are 11 coefficients appearing in Table 2, not to mention such numbers as $\eta'$ and $\eta''$. Also note that the values of these coefficients are different for the initially contractive and dilative sand. Therefore, there are altogether 22 coefficients which should be determined experimentally. A large number of various coefficients is a common problem in soil mechanics. Probably some of these coefficients are correlated but there is still lack of empirical data to find possible correlations. Some researchers construct models which have "a minimal set of parameters", but description of a bare set of experimental data certainly needs more than a few numbers, as shown in Section 3. Nevertheless, the problem of minimisation of material parameters remains an important research question in soil mechanics.

Table 3 summarises the respective functions for the case of unloading, after Sawicki and Świdziński (2007). The shape of these functions is similar for both dilative and contractive states of sand, but the parameters are obviously different.

**Table 3.** Functions appearing in Eqs. (4.1) for the case of unloading

| Function | | | |
|---|---|---|---|
| $M$ | $N$ | $P$ | $Q$ |
| $\dfrac{A_v^u}{2\sqrt{p'}}$ | $\dfrac{a_v}{\sqrt{p'}}$ | $\dfrac{A_q^u}{2\sqrt{p'}}$ | $\dfrac{b_q}{\sqrt{p'}}$ |

The values of $A_v^u$ and $A_q^u$ are given in Section 3. The remaining coefficients are the following: $a_v = -0.87$ and $-0.39$ for the initially loose and dense sand respectively; $b_q = 0.76$ and $0.4$ for a loose and dense sand.

## 5.  3D form of incremental equations

Incremental equations (4.1) are formulated for the specific configuration corresponding to the experiments performed in triaxial conditions. The stress and strain variables, i.e. $p'$, $q$, $\varepsilon_v$ and $\varepsilon_q$, appearing in these equations are related to the invariants of respective tensors, as shown in Section 2.1. These relations enable generalization of these equations to a 3D form, using the methods of tensor algebra.

Such a method of derivation of constitutive equations is different from the approach suggested in already classical publications, where the starting point

are the tensor relations expressed in a most general form. Then the shape of these equations is simplified according to the problem analysed, see Sawczuk and Stutz (1968), Boehler and Sawczuk (1970, 1977) or Betten (1988).

It is assumed that the general form of the incremental equations is the following, see Sawicki (2008)

$$d\varepsilon_v = Adp' + BdJ_2 \qquad\qquad d\boldsymbol{\varepsilon}^{dev} = \mathbf{C}dp' + Dd\boldsymbol{\sigma}'^{dev} \tag{5.1}$$

where $A$, $B$ and $D$ are some scalar functions which depend on the invariants of the effective stress tensor. $\mathbf{C}$ is a tensor that depends on the current stress state and the kind of initial anisotropy of sand. The quantities $J_2$, $\boldsymbol{\varepsilon}^{dev}$ and $\boldsymbol{\sigma}'^{dev}$ are defined in Eqs. (2.2)$_3$ and (2.3), respectively.

The structure of Eqs. (5.1) displays decomposition of the spherical and deviatoric parts of the stress and strain tensors. Experimental results show that the sand exhibits cross-isotropic behaviour, with the vertical axis indicating the privileged direction. In order to take into account this effect, the following structural tensor is introduced

$$\mathbf{S} = \begin{bmatrix} 1 & 0 & 0 \\ 0 & 0 & 0 \\ 0 & 0 & 0 \end{bmatrix} \tag{5.2}$$

Assume that

$$\mathbf{C} = C\mathbf{S}^{dev} \tag{5.3}$$

where $C$ is a scalar function and

$$\mathbf{S}^{dev} = \frac{1}{3}\begin{bmatrix} 2 & 0 & 0 \\ 0 & -1 & 0 \\ 0 & 0 & -1 \end{bmatrix} \tag{5.4}$$

The functions $A$, $B$, $C$ and $D$ are determined from the conditions that Eqs. (5.1) reduce to Eqs. (4.1) in the case of triaxial compression tests. It can easily be checked, by substitution, that the following relations are valid

$$A = M \qquad B = \frac{N\sqrt{3}}{2\sqrt{J_2}} \qquad C = \frac{3P}{2} \qquad D = \frac{3Q}{2} \tag{5.5}$$

In the same way, the other relations can be generalized. The criterion of spherical loading/unloading remains unchanged, but in the case of deviatoric loading/unloading one should substitute the following value of the non-dimensional stress increment into the respective condition, (i.e. $d\eta > 0/d\eta < 0$)

$$d\eta = \frac{1}{p'}(dq - \eta dp') = \frac{\sqrt{3}}{p'}\Big(\frac{1}{2\sqrt{J_2}}dJ_2 - \frac{\sqrt{J_2}}{p'}dp'\Big) \tag{5.6}$$

The instability condition (2.6) takes the following form

$$J_2 = \frac{1}{3}\Psi^2 (p')^2 \tag{5.7}$$

## 6.   Undrained behaviour

Constitutive incremental equations (4.1), or more general relations (5.1), describe also the behaviour of saturated sand in undrained conditions. Such conditions take place in the case of rapid loads as those during earthquakes, explosions and other dynamic excitations. In such circumstances, there is no time for excess pore-pressure to dissipate. The undrained conditions can also be investigated in a laboratory, as the construction of triaxial apparatus may prevent the outflow of pore water. Practically, the undrained conditions are identified with the condition of zero volumetric changes, i.e.

$$d\varepsilon_v = 0 \tag{6.1}$$

Equations $(4.1)_1$ and (6.1) lead to the following formula

$$Mdp' + Ndq = 0 \tag{6.2}$$

Recall that $dp' = dp - du$, where $dp$ is the increment of the total mean stress, and $du$ – increment of pore-pressure. Therefore, Eq. (6.2) can be rewritten as

$$du = dp + \frac{N}{M}dq \tag{6.3}$$

A similar procedure applies to Eqs. $(5.1)_1$ and (6.1). Recall that the functions $N$ and $M$ depend on $p' = p - u$, see Table 2. Integration of Eq. (6.3) for a given total stress history leads to corresponding histories of pore-pressure and effective stresses. Some important examples will be presented in Part II of this paper.

In the case of a compressible fluid, i.e. of pore water containing some admixture of gas, Eq. (6.3) should be modified. Simple analysis leads to the equivalent form of this equation, see Sawicki and Świdziński (2007)

$$du = \frac{1}{M + n_0\kappa_f}(Mdp + Ndq) \tag{6.4}$$

where $n_0$ is the initial porosity; $\kappa_f$ – pore fluid compressibility.

## 7.  Conclusions

The results reported in this paper can be summarised as follows:

  a) The existing models of granular soils do not always lead to realistic predictions of the pre-failure behaviour of those materials. There is still a need for the models which would better reproduce the real response of sand and such with a rather simple formal structure.

  b) The model proposed in this paper is based on the analysis of bare empirical data, and its structure is relatively simple. Such a model can be easily applied to solve practical problems.

  c) The model proposed takes into account some features which have been ignored in traditional soil mechanics as, for example, steady state line, instability line, initially dilative or contractive states and initial anisotropy.

  d) The model derived firstly for fully drained conditions is also valid for undrained conditions, which will be shown in Part II of this paper.

## References

1. Betten J., 1988, Application of tensor functions to the formulation of yield criteria for anisotropic materials, *Int. Journal of Plasticity*, **4**, 29-46

2. Boehler J.P., Sawczuk A., 1970, Équilibre limite des sols anisotropes, *Journal de Mécanique*, **9**, 1, 5-33

3. Boehler J.P., Sawczuk A., 1977, On yielding of oriented solids, *Acta Mechanica*, **27**, 185-206

4. Bolton M., 2001, The role of micro-mechanics in soil mechanics, Technical Report CUED/D-Soils/TR313, University of Cambridge

5. Głębowicz K., 2006, Hypoplastic modelling of pre-failure behaviour of sand against experimental data, *Arch. of Hydro-Engineering and Environ. Mech.*, **53**, 1, 31-47

6. Kolymbas D., 2000a, Introduction to hypoplasticity, *Advances in Geotechnical Engineering and Tunnelling*, Balkema, Rotterdam/Brookfield

7. KOLYMBAS D., 2000b, The misery of constitutive modelling, In: *Constitutive Modelling of Granular Materials*, D. Kolymbas (Edit.), Springer, Berlin-Heidelberg-New York, 11-24

8. MENZIES B.K., 1988, A computer controlled hydraulic triaxial testing system, *ASTM*, **977**, 82-94

9. POULOS S.J., 1981, The steady state of deformation, *J. Geotech. Engrg. ASCE*, **107**, GT5, 501-516

10. SAADA A., BIANCHINI G. (EDIT.), 1987, Constitutive equations for granular non-cohesive soils, *Proc. of Int. Workshop*, Cleveland, Balkema, Rotterdam/Brookfield

11. SAWCZUK A., STUTZ P., 1968, On formulation of stress-strain relations for soils at failure, *Journal of Applied Mathematics and Physics (ZAMP)*, **19**, 5, 770-778

12. SAWICKI A., 2003, Cam-clay approach to modelling pre-failure behaviour of sand against experimental data, *Arch. of Hydro-Engineering and Environ. Mech.*, **50**, 3, 239-249

13. SAWICKI A., 2008, 3D and 2D formulation of incremental stress-strain relations for granular soils, *Arch. of Hydro-Engineering and Environ. Mech.*, **55**, 1, 45-53

14. SAWICKI A., ŚWIDZIŃSKI W., 2007, Drained against undrained behaviour of granular soils, *Arch. of Hydro-Engineering and Environ. Mech.*, **54**, 3, 207-222

15. ŚWIDZIŃSKI W., MIERCZYŃSKI J., 2002, On the measurement of axial strains in the triaxial test, *Arch. of Hydro-Engineering and Environ. Mech.*, **49**, 1, 23-41

16. ZIENKIEWICZ O., CHAN A., PASTOR M., SCHREFLER B., SIMONI T., 1999, *Computational Geomechanics with Special Reference to Earthquake Engineering*, J. Wiley & Sons, Chichester

17. ŻYCZKOWSKI M., 1973, *Complex Loads in Plasticity Theory*, PWN, Warsaw [in Polish]

## Związki naprężenie-odkształcenie dla piasków suchych i nawodnionych Część I: Model przyrostowy

### Streszczenie

Zaproponowano model przyrostowy opisujący zachowanie się gruntów sypkich przed osiągnięciem stanu granicznego. Równania konstytutywne wyprowadzono bezpośrednio ze związków naprężenie-odkształcenie, otrzymanych z badań trójosiowych.

W modelu uwzględniono początkową anizotropię gruntu, jego stan początkowy (dylatywny lub kontraktywny) oraz linię niestabilności. Równania przyrostowe zostały uogólnione na przypadek trójwymiarowy, zgodnie z regułami algebry tensorowej. Model zastosowano do symulacji zachowania się nawodnionego gruntu w warunkach bez odpływu wody z porów, co prowadzi między innymi do zjawiska upłynnienia. Przedstawione podejście jest alternatywą do modeli sprężysto-plastycznych oraz hipoplastycznych. Część I pracy dotyczy sformułowania modelu i jego kalibracji, a w części II przedstawiono predykcje modelu, które porównano z wynikami doświadczeń.